

## Non-local collisionless and collisional electron transport in low-temperature plasma

This article has been downloaded from IOPscience. Please scroll down to see the full text article.

2009 Plasma Phys. Control. Fusion 51 124003

(<http://iopscience.iop.org/0741-3335/51/12/124003>)

View [the table of contents for this issue](#), or go to the [journal homepage](#) for more

Download details:

IP Address: 198.35.3.245

The article was downloaded on 25/06/2010 at 15:18

Please note that [terms and conditions apply](#).

# Non-local collisionless and collisional electron transport in low-temperature plasma

I D Kaganovich<sup>1</sup>, V I Demidov<sup>2,3</sup>, S F Adams<sup>4</sup> and Y Raitsev<sup>1</sup>

<sup>1</sup> Princeton Plasma Physics Laboratory, Princeton, NJ 08543, USA

<sup>2</sup> UES, Inc., 4401 Dayton-Xenia Rd, Dayton, OH 45432, USA

<sup>3</sup> West Virginia University, Morgantown, WV 26506, USA

<sup>4</sup> Air Force Research Laboratories, Wright-Patterson AFB, OH 45433, USA

E-mail: [ikaganov@pppl.gov](mailto:ikaganov@pppl.gov)

Received 17 June 2009, in final form 15 July 2009

Published 10 November 2009

Online at [stacks.iop.org/PPCF/51/124003](http://stacks.iop.org/PPCF/51/124003)

## Abstract

This paper reviews recent advances in non-local electron kinetics in low-pressure discharges. Non-local electron kinetics, non-local electrostatics with collisionless electron heating and non-linear processes in the sheaths are typical for such discharges. Progress in understanding the non-local interaction of electric fields with real, bounded plasma created by the fields has been one of the major achievements of the past few decades.

(Some figures in this article are in colour only in the electronic version)

## 1. Introduction

The purpose of this paper is to facilitate discussion on non-local, collisionless and collisional phenomena in low-pressure plasmas between scientific communities working on high-temperature, fusion plasmas and low-temperature, gas-discharge plasmas. Such low-pressure plasmas have remarkable characteristics: changing conditions in one place may lead to unexpected changes in plasma properties far away in another part of the plasma. Low-pressure discharges are widely used as the plasma sources for a variety of plasma applications, including plasma processing, discharge lighting, sources for particle beams and nanotechnology [1, 2]. Another growing and important application of low-pressure plasmas is the plasma thrusters for satellite propulsion [3]. The production of low-temperature plasmas with controllable parameters, including the plasma density, the electron temperature and the electron and ion energy distribution functions is one of the critical challenges of modern plasma engineering. Optimization of plasma parameters necessitates basic research with the main objective of developing sophisticated modeling capabilities to capture the key processes in the plasma and plasma-wall interactions.

The distinctive property of plasmas of these discharges is that such plasmas are always in a non-equilibrium state: the electrons are not in thermal equilibrium with the neutral species and ions, in view of the fact that the electron mean energy is typically much larger than the mean energy of the ions and neutrals. Moreover, the electrons are also not in thermodynamic equilibrium within their own ensemble, which results in a significant departure of the electron velocity distribution function (EVDF) from a Maxwellian EVDF—the EVDF may have a complex form and sometimes can be noticeably anisotropic. In low-pressure gas-discharge plasmas, the electron mean free path can be comparable to or larger than scales of the plasma density profile and of the electromagnetic field inhomogeneity. Therefore, in its thermal motion, an electron can move between collisions sampling different values of electric field along its trajectory. As a result, the electron current at some point in the plasma is determined not by the local value of the electric field, but by the entire profile of the electric field. Non-local electron kinetics, non-local electrodynamics with collisionless electron heating and non-linear processes in the sheaths are typical for such plasmas. These non-equilibrium conditions make gas-discharge plasmas a remarkable tool for plasma applications, because they provide considerable freedom to choose optimal plasma properties.

Progress in understanding the interaction of electromagnetic fields, with a real, bounded plasma created by this field and the resulting changes in the structure of the applied electromagnetic field, has been one of the major achievements of the past few decades. The Workshop on Non-local, Collisionless Electron Transport in Plasmas has updated and summarized the progress in the topic and discussed future directions in the field. Invited papers from the workshop have been published in the special issue of IEEE Transactions on Plasma Science [4]. The purpose of this paper is to briefly review recent advances in non-local electron kinetics and transport in gas-discharge plasmas and give a number of examples where non-locality effects are important.

The paper is focused on plasmas with the presence of energetic electrons with energies much greater than the mean energy of all electrons. The non-local effects in such plasmas are especially well pronounced, because a small fraction of energetic electrons can lead to significant changes in plasma and sheath properties. Therefore, by controlling a small group of energetic electrons, e.g. from the plasma boundaries, effective control over plasma properties is achievable.

The paper is organized as follows. Section 2 considers a collisionless plasma, where the electron mean free path is large compared with the typical scale of discharge gap or a scale of the electric field profile. Two practical examples of Hall thruster plasma and anomalous skin effect in radio-frequency discharges are described. Section 3 is devoted to a collisional plasma, where the electron mean free path is small compared with the typical scale of the discharge gap, but the electron energy relaxation length is large compared with the discharge gap. Section 4 gives conclusions.

## **2. Non-local electron kinetics in collisionless plasma**

### *2.1. Kinetic effects in Hall thruster discharge*

The plasma thrusters for satellite propulsion utilize very low-pressure plasmas [3], where the electron mean free path is typically a hundred times larger than the discharge gap. As a result, the typical assumption of the fluid theories that the EVDF is a Maxwellian is incorrect. Results of particle-in-cell (PIC) simulations showed that the EVDF is not a Maxwellian—it is strongly anisotropic, depleted at high energies, and in some cases, even non-monotonic [5, 6], as shown, for example, in figure 1. The average kinetic energy of electron motion in the

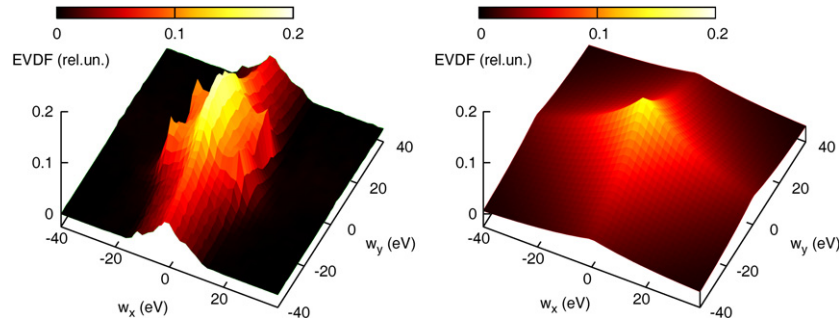


**Figure 1.** Complex structure of a strongly anisotropic EVDF in the channel of a Hall thruster discharge (left) versus an isotropic Maxwellian EVDF (right). Simulations were performed for the electric field  $E_z = 200 \text{ V cm}^{-1}$ , magnetic field  $B_x = 100 \text{ G}$ , discharge gap  $L = 2 \text{ cm}$ , gas density  $N = 10^{18} \text{ m}^{-3}$ , turbulent collision frequency  $\nu = 7 \times 10^5 \text{ s}^{-1}$ , EVDF in PIC simulations has effective electron temperature  $T_x = 11.1 \text{ eV}$ ,  $T_z = 31.9 \text{ eV}$ , a Maxwellian EVDF  $T_x = T_z = 25 \text{ eV}$ . More details are available in [5, 6].

direction parallel to the walls is several times larger than the average kinetic energy of electron motion in the direction normal to the walls. Because of the significant departure of the EVDF from a Maxwellian, the kinetic simulations give rather different results for plasma properties than conventional fluid calculations based on a Maxwellian EVDF. For example, the sheath potential is typically estimated in fluid theories to be several, from 3 to 5, electron temperatures. The PIC simulations and kinetic theory [5, 6] calculate the sheath potential to be much smaller, of the order of one electron temperature. This is due to the presence of a large loss cone in the phase space; all electrons with energy above the electron potential energy corresponding to the wall potential,  $-e\Phi_w$ , leave the plasma and are not replenished quickly enough. The electron flux to the wall is determined by electron collisions which scatter electrons into the loss cone from the phase space outside the loss cone. Therefore, the electron flux to the wall is proportional to the collision frequency and is small compared with the estimates provided by the fluid theory.

In a Hall thruster, the typical electron energy can reach up to 100 eV [7]. Energetic electrons striking the wall can emit one or two secondary electrons and the flux of emitted electrons can be greater than the flux of primary electrons. In typical plasmas the wall is charged negatively to prevent large electron flux to the wall. Intense electron emission from the wall can significantly reduce the wall potential. Such reduction in the wall potential leads to an increase in the electron flux to the wall of primary hot electrons and can cause undesired heating of the walls and even wall material evaporation. The accurate analysis of the wall potential also has to be performed kinetically, because the secondary electrons form two beams propagating between the walls of a thruster channel in opposite radial directions and cannot be described by a Maxwellian EVDF as shown in figure 1. The cold secondary electron flux from the opposite wall can also reach the wall and reduce the emitted flux. Therefore, the flux of secondary electrons from the opposite wall has to be taken into account. The counter propagating electron fluxes can be subject to the two-stream instability [5]. All these effects require kinetic treatment and cannot be described even qualitatively correctly in the fluid approximation based on a Maxwellian EVDF. For example, kinetic treatment predicts very little effect of intense secondary electron emission on energy losses and a strong effect on electron cross magnetic field conductivity [6] in agreement with experimental data [7], whereas the modeling making use of the fluid approximation makes an opposite prediction.

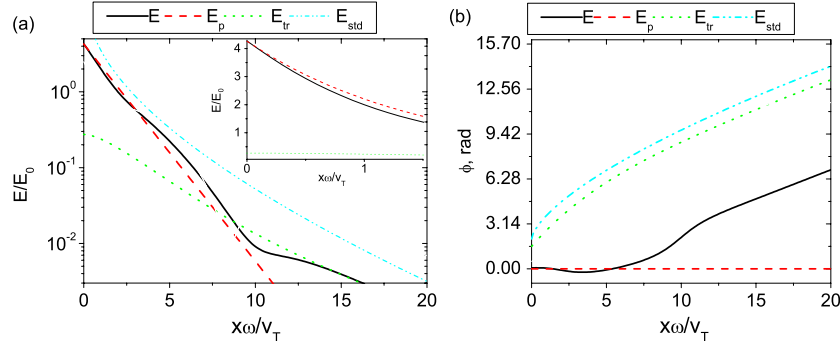


**Figure 2.** Plot of the rf electric field as a function of normalized coordinate  $x\omega/V_T$  for plasma parameters  $n = 10^{11} \text{ cm}^{-3}$ ,  $T = 3 \text{ eV}$ ,  $f = 13.56 \text{ MHz}$ . Shown are (a) amplitude and (b) phase. Solid lines show the exact electric field profile  $E(x)$ , dashed (red) line—the exponential part of the electric field  $E_p(x) = E_0 \exp(-k_p x)$ , dotted line (green) the difference of two  $E_t(x)$  and chain (cyan) line  $E_{std}(x)$  shows the asymptotic calculation for transient part  $E_t$  [10].

## 2.2. Anomalous skin effect in radio-frequency discharges

Another example of non-local electron kinetic phenomena is the anomalous skin effect in radio-frequency (rf) low-pressure discharges, which are sustained by the applied rf frequency 1–100 MHz voltage. For a review of the anomalous skin effect see, for example, [8, 9]. A radio-frequency electromagnetic wave does not penetrate into a plasma if the wave frequency  $\omega$  is smaller than the electron plasma frequency  $\omega_p = \sqrt{4\pi e^2 n_e / m}$ , where  $e$  and  $m$  are the electron charge and mass, respectively, and  $n_e$  is the electron density. Electrons distribute their charge and current to shield out the electromagnetic wave. The shielding depends on the direction of the wave with regard to the plasma boundary. If the wave electric field is directed perpendicularly to the plasma boundary (capacitive coupling), the rf field penetrates into the plasma only within a depth of the order of the Debye length  $v_T/\omega_p$ , where  $v_T = \sqrt{2kT_e/m}$  is the electron thermal velocity, determined by the electron temperature  $T_e$ . If the wave electric field is directed along the plasma boundary (inductive coupling), the rf field penetrates into the plasma only within a depth of the order of the skin depth  $c/\omega_p$ , where  $c$  is the speed of light in vacuum. Here, we consider collisionless plasma where the collision frequency is small,  $\nu \ll \omega$ , and the electrons undergo rare collisions during the rf cycle, thus, collisions have little effect on wave screening by the plasma. The other important scale is the phase-mixing scale,  $v_T/\omega$ , which determines the typical width of the electron return current in the plasma. For both wave directions it was found that the electric field profile consists of two parts: the major part of the electric field profile decays with a scale given by the Debye length for capacitive discharge or the skin depth for inductive discharge. However, there are long tails of the rf electric profile which decay on a scale of  $v_T/\omega$ , as shown in figure 2 [10]. Such deep penetration of the rf electric field occurs due to thermal electron motion, in which the electrons transport an acquired velocity kick into the plasma where the velocity kicks acquired at different times eventually phase mix. In [10] it is shown that separating the electric field profile into exponential and non-exponential parts yields an efficient qualitative and quantitative description of the anomalous skin effect.

An interesting effect that can lead to enhanced heating for bounded, low-pressure plasmas is a bounce resonance between the frequency  $\omega$  of the driving rf field and the frequency  $\Omega_b$  of the bounce motion of the plasma electrons confined to the potential well by an electrostatic ambipolar potential  $\phi(x)$  and the sheath electric fields near the plasma edges [11]. In the

collisionless limit where the discharge gap is small compared with the electron mean free path the heating rate may depend on collision frequency [12], when the decorrelation time between interactions with rf field is longer than the time between collisions. This effect is similar in nature to the dependence of the electron flux to the wall on collision frequency discussed in the previous section. In both cases the effect is proportional to the small collision frequency even though the mean free path is large and the main electron dynamics is collisionless.

### 3. Non-local electron kinetics in collisional plasma

In collisional plasmas the electron mean free path is small compared with the discharge gap; therefore, the electron momentum acquired from the electric field dissipates into the thermal energy, and the electron velocity distribution is close to an isotropic EVDF [13]. However, electron energy losses in collision with an atom constitute only a small fraction of its initial energy (of order  $2m/M$ , where  $M$  is the atom mass). The energy relaxation length is given by the distance the electron propagates before it loses a substantial part of its energy. For elastic collisions the energy relaxation length,  $\lambda_\epsilon$ , is a factor of  $\sqrt{M/m}$  larger than the electron mean free path  $\lambda$  [13, 14]. The mean free path with respect to the electron–electron collisions is typically large compared with the energy relaxation length in partially ionized plasmas and the electrons do not reach equilibrium, i.e. the EVDF is a non-Maxwellian [15]. In collisionless plasmas, described in the previous sections, the EVDF can be non-Maxwellian in partially or fully ionized plasmas. In collisional plasmas the EVDF can be non-Maxwellian only in partially ionized plasmas with a small degree of ionization because the rate of electron–electron collisions has to be small compared with other processes affecting the EVDF formation.

If the discharge dimension is small compared with the energy relaxation length, the EVDF has to be described by a non-local model, i.e. it depends on the entire profile of the electric field and not on the local value of the electric field [13, 14, 16–18]. Because the EVDF is non-Maxwellian and the electron–electron collision rate is small compared with the heating rate or energy losses in inelastic collisions, electrons tend to stratify into different groups depending on their origin, confinement or heating mechanisms. These non-equilibrium conditions provide considerable freedom to choose optimal plasma parameters for applications, which make gas-discharge plasmas remarkable tools for a variety of plasma applications, including plasma processing, discharge lighting, plasma propulsion, particle beam sources and nanotechnology. In the following we explore the coupling between the non-Maxwellian EVDF and the wall potential. Because the wall potential determines the electron wall losses and depletion of the energetic part of the EVDF, the value of the wall potential greatly affects the tail of the EVDF. On the other hand, only energetic electrons reach the wall and the current to the wall can be used as effective and robust discharge diagnostics [19]. If the wall is floating, the wall potential is determined by a balance between the electron and ion fluxes. The electron flux is highly sensitive to the number of energetic electrons. Adding a small number of energetic electrons can greatly influence the wall potential and allows for effective control of the wall potential. In the case of a Maxwellian EVDF, the wall potential is determined by the plasma electron temperature, typically  $-e\Phi_w = 3 - 5kT_e$  depending on the gas. However, if a small fraction of energetic electrons is present so that their flux is large compared with the ion flux, the wall potential is determined by the energetic electron energy. If the energetic electron energy is large compared with the electron temperature, the wall will be charged by these energetic electrons to the larger values of the potential. This effect was observed in experiments in the discharge afterglow [20, 21]. In the discharge afterglow, the plasma density decays due to wall losses and recombination. The electron temperature decreases much faster than the plasma density

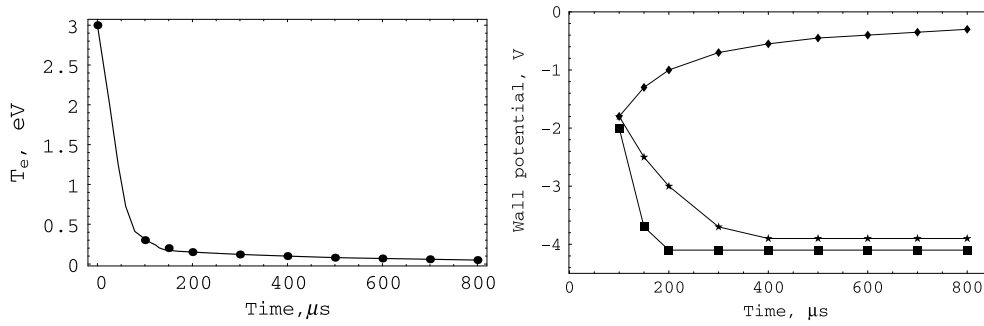


**Figure 3.** The electron temperature (left, dots show experimental data) and the wall potential in xenon afterglow plasma (stars show experimental data, diamonds show calculation without fast electrons and squares indicate the calculations taking the fast electrons into account) [20, 21].

due to evaporative cooling and elastic collisions with atoms. The electron energy decreases from several electronvolts in the active phase of the discharge, when a maintaining voltage is applied, to energy of the order of 0.1 eV in the afterglow [22], see figure 3. Typically, the wall potential monotonically decreases proportionally to the electron temperature. However, experiments showed that at a certain time the wall potential stops decreasing with time and can even increase during a certain time interval, see figure 3. Such a drastic change in the behavior of the wall potential occurs due to the presence of the energetic electrons with energy much larger than the bulk electron energy in the afterglow,  $\varepsilon_f \gg kT_e \sim 0.1$  eV. Energetic electrons  $e'$  in the afterglow can arise in a number of physical and chemical processes. These processes include the superelastic collisions with participation of excited atoms  $A^*$  and slow electrons  $e$  ( $A^* + e \rightarrow A + e'$ ), the Penning ionization ( $A^* + A^* \rightarrow A + A^+ + e'$ ), photoionization ( $A^* + h\nu \rightarrow A^+ + e'$ ) and the associative detachment ( $A^- + A \rightarrow A_2 + e'$ ) [23]. The energy of the produced electrons in these processes depends on the specific atom or molecule involved and usually lies in the range from a few electronvolts to 20 eV. As soon as the flux of the energetic electrons becomes large compared with the ion flux, the wall potential is predominantly determined by energetic electrons and its value increases or stays nearly constant, see figure 3 [20, 21].

Energetic electrons can also be injected into the plasma from the emitting walls or grids. As an example, we studied the dependence of the wall potential in the direct current discharges with hot and cold cathodes. Figure 4 shows the schematic of an experimental device with a cold cathode and the wall potential dependence on gas pressure. Making use of the PIC simulations the wall potential dependence on gas pressure can be explained by changes in fluxes of energetic electrons to the wall.

A drawing of the discharge device with a hot cathode and a diaphragm is shown in figure 5. The diaphragm electrode was used to change the discharge properties. Experiments demonstrated that the application of an additional voltage to the diaphragm can create two completely different discharge regimes. In the first regime the plasma glow fills the volume between the cathode and the diaphragm. In the second regime the glow between the cathode and the diaphragm is absent, but there is a bright glow in close proximity to the diaphragm opening. Typical profiles of plasma potential for both regimes are shown in figure 5. The observed sharp transition between regimes can be again explained by changes in fluxes of fast electrons.

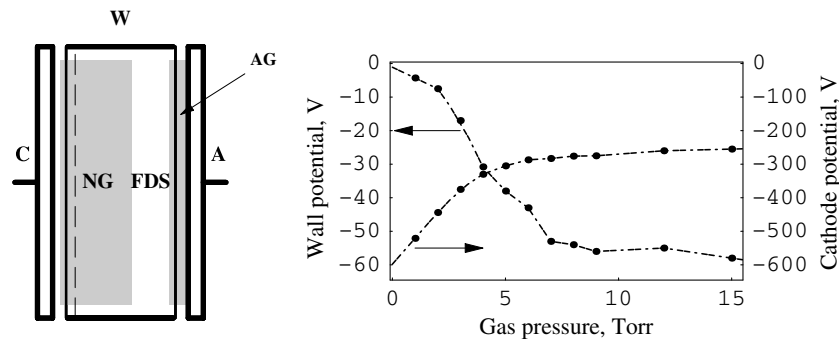


**Figure 4.** Schematic diagram of experimental device of dc discharge with cold cathode consisting of cathode (C), anode (A) and cylindrical wall (W). Typical structures of the discharge plasma are the negative and anode glows, NG and AG, respectively, and Faraday dark space FDS [24]. The cathode sheath boundary is indicated by the dashed line. Typical results of the floating wall,  $V_w$ , and cathode,  $V_c$ , potential as a function of argon gas pressure and a discharge current of 3 mA.

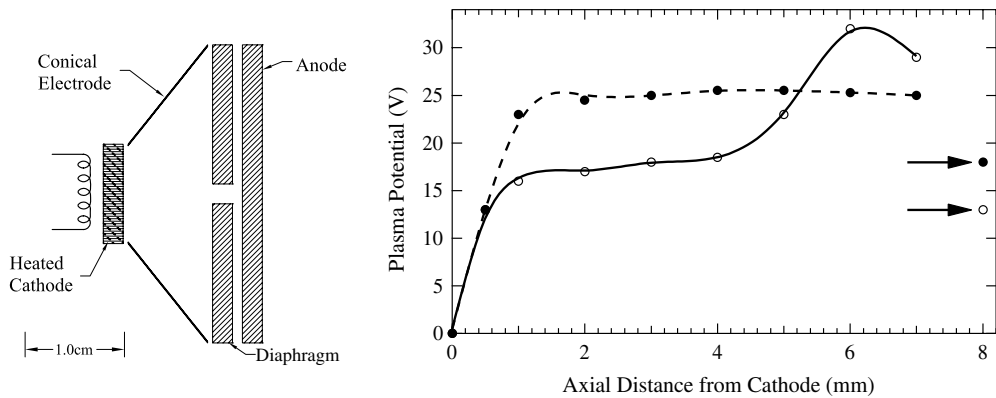


**Figure 5.** (Left) Schematic diagram of the experimental device of dc discharge with hot cathode. (Right) Axial profile of the plasma potential for voltage on diaphragm 13 V and 18 V. Arrows indicate diaphragm potentials [25].

#### 4. Conclusions

A distinctive property of low-temperature plasmas is that such plasmas are often in a non-equilibrium state: the electrons are not in thermal equilibrium with the neutral species and ions, and the electrons are also not in thermodynamic equilibrium within their own ensemble, which results in a significant departure of the EVDF from a Maxwellian. These non-equilibrium conditions provide considerable freedom to choose optimal plasma parameters for applications, which make gas-discharge plasmas remarkable tools for a variety of plasma applications, including plasma processing, discharge lighting, plasma propulsion, particle beam sources and nanotechnology. Typical phenomena in such discharges include non-local electron kinetics, non-local electrodynamics with collisionless electron heating and non-linear kinetic processes of the plasma-wall interactions and the space charge sheath formation. It was shown experimentally and in PIC simulations that controlling a small number of energetic electrons with auxiliary electrodes and voltage forms can significantly affect plasma properties.

## Acknowledgments

This work was supported by The Air Force Office of Scientific Research.

## References

- [1] Lieberman MA and Lichtenberg AJ 1994 *Principles of Plasma Discharges and Materials Processing* (New York: Wiley)
- [2] Chen F F and Chang J P 2003 *Lecture Notes on Principles of Plasma Processing* (New York: Kluwer)
- [3] Morozov A I and Savelyev V V 2000 *Review of Plasma Physics* vol 21 ed by B B Kadomtsev and V D Shafranov (New York: Consultants Bureau) p 203  
Zhurin V V, Kaufman H R and Robinson R S 1999 *Plasma Sources Sci. Technol.* **8** 1  
Martinez-Sanchez M and Pollard J E 1998 *Propul. Power* **14** 688  
Adam J C *et al* 2008 *Plasma Phys. Control. Fusion* **50** 124041
- [4] 2006 Special Issue on Nonlocal, collisionless electron transport in plasmas *IEEE Trans. Plasma Sci.* **34** (details of the workshop can be found at <http://w3.pppl.gov/~ikaganov/PPPL2005/>)
- [5] Sydorenko D, Smolyakov A, Kaganovich I and Raitsev Y 2006 *IEEE Trans. Plasma Science* **34** 895  
Sydorenko D, Smolyakov A, Kaganovich I and Raitsev Y 2006 *Phys. Plasmas* **13** 014501  
Sydorenko D, Smolyakov A, Kaganovich I and Raitsev Y 2007 *Phys. Plasmas* **14** 013508  
Sydorenko D, Smolyakov A, Kaganovich I and Raitsev Y 2008 *Phys. Plasmas* **15** 053506
- [6] Kaganovich I D, Raitsev Y, Sydorenko D and Smolyakov A 2007 *Phys. Plasmas* **14** 057104
- [7] Raitsev Y, Smirnov A, Staack D and Fisch N J 2006 *Phys. Plasmas* **13** 014502
- [8] Kolobov V I and Economou D J 1997 *Plasma Sources Sci. Technol.* **6** R1
- [9] Godyak V A 2005 *Phys. Plasmas* **12** 055501
- [10] Kaganovich I D, Polomarov O V and Theodosiou C E 2006 *IEEE Trans. Plasma Science* **34** 696  
Kaganovich I D, Polomarov O V and Theodosiou C E 2004 *Phys. Plasmas* **11** 2399  
Kaganovich I D 2002 *Phys. Rev. Lett.* **89** 265006
- [11] Kaganovich I D, Kolobov V I and Tsendin L D 1996 *Appl. Phys. Lett.* **69** 3818  
Aliev Yu M, Kaganovich I D and Schluter H 1997 *Phys. Plasmas* **4** 2413  
Polomarov O V *et al* 2006 *IEEE Trans. Plasma Sci.* **34** 767  
Polomarov O V *et al* 2005 *Phys. Plasmas* **12** 104505
- [12] Kaganovich I D 1999 *Phys. Rev. Lett.* **82** 327
- [13] Kaganovich I D and Tsendin L D 1992 *IEEE Trans. Plasma Sci.* **20** 66
- [14] Tsendin L D 2009 *Plasma Sources Sci. Technol.* **18** 014020
- [15] Godyak V A 2006 *IEEE Trans. Plasma Sci.* **34** 755
- [16] Tsendin L D 1995 *Plasma Sources Sci. Technol.* **4** 200
- [17] Kolobov V I and Godyak V A 1995 *IEEE Trans. Plasma Sci.* **23** 503
- [18] Kortshagen U, Busch C and Tsendin L D 1996 *Plasma Sources Sci. Technol.* **5** 1
- [19] Demidov V I, Blessington J, Adams S F, Kaganovich I and Williamson J M 2009 *36th EPS Conf. on Plasma Physics (Sofia, Bulgaria, 29 June–3 July 2009)* <http://eps2009.uni-sofia.by/>
- [20] Demidov V I, DeJoseph C A Jr and Kudryavtsev A A 2005 *Phys. Rev. Lett.* **95** 215002
- [21] Demidov V I, DeJoseph C A Jr, Blessington J and Koepke M E 2007 *Europhys. News* **38** 21
- [22] Arslanbekov R R, Kudryavtsev A A and Tsendin L D 2001 *Phys. Rev. E* **64** 016401
- [23] Blagoev A B, Kolokolov N B and Kudryavtsev A A 1994 *Phys. Scr.* **50** 371
- [24] Kolobov V I and Tsendin L D 1992 *Phys. Rev. A* **46** 7837
- [25] Demidov V I, DeJoseph C A Jr and Simonov V Ya 2007 *Appl. Phys. Lett.* **91** 201503